

The physics models of FLUKA: status and recent developments

A. Fassò*, A. Ferrari†, S. Roesler

CERN, Geneva, CH-1211 Switzerland

P.R. Sala†

ETH Zürich, CH-8093 Zürich, Switzerland

F. Ballarini, A. Ottolenghi

Università degli Studi di Pavia and INFN, via Bassi 6, I-27100, Pavia, Italy

G. Battistoni, F. Cerutti, E. Gadioli, M.V. Garzelli

Università degli Studi di Milano and INFN, via Celoria 16, I-20133, Milan, Italy

A. Empl

Houston University, Texas, USA

J. Ranft

Siegen University, Germany

A description of the intermediate and high energy hadronic interaction models used in the FLUKA code is given. Benchmarking against experimental data is also reported in order to validate the model performances. Finally the most recent developments and perspectives for nucleus–nucleus interactions are described together with some comparisons with experimental data.

1. Generalities

FLUKA [1, 2, 3, 4] is a multipurpose transport Monte Carlo code, able to treat hadron–hadron, hadron–nucleus, neutrino, electromagnetic, and μ interactions up to 10000 TeV. Charged particle transport (handled in magnetic field too) includes all relevant processes [1]. About nucleus–nucleus collisions, since ion–ion nuclear interactions were not yet treated in FLUKA, past results have been obtained in the superposition model approximation, where primary nuclei (0–10000 TeV/A) were split into nucleons before interacting. With the integration of ion interaction codes (see Section 4) and the cross section parameterization, this approximation is now obsolete.

FLUKA is based, as far as possible, on original and well tested microscopic models. Due to this “microscopic” approach to hadronic interaction modelling, each step is self-consistent and has solid physical bases. Performances are optimized comparing with particle production data at single interaction level. No tuning whatsoever is performed on “integral” data, such as calorimeter resolutions, thick target yields, etc. Therefore, final predictions are obtained with a minimal set of free parameters, fixed for all energies and target/projectile combinations. Results in complex cases as well as scaling laws and properties come forth naturally from the underlying physical models and the basic conservation laws are fulfilled *a priori*.

*on leave from GSI, Darmstadt, Germany (Present address: SLAC, P.O. Box 4349, MS 48, Stanford, CA 94309, USA)

†on leave from INFN, Sezione di Milano, via Celoria 16, I-20133, Milan, Italy

2. Hadron–nucleon interaction models

A comprehensive understanding of hadron–nucleon (h–N) interactions over a wide energy range is of course a basic ingredient for a sound description of hadron–nucleus ones. Elastic, charge exchange and strangeness exchange reactions are described as far as possible by phase–shift analysis and/or fits of experimental differential data. Standard eikonal approximations are often used at high energies.

At the low energy end (below 100 MeV) the p–p and p–n cross sections are rapidly increasing with decreasing energy. The n–p and the p–p cross sections differ by about a factor three at the lowest energies, as expected on the basis of symmetry and isospin considerations, while at high energies they tend to be equal.

The total cross section for the two isospin components present in the nucleon–nucleon amplitude is given by:

$$\begin{aligned}\sigma_1 &= \sigma_{pp} \\ \sigma_0 &= 2\sigma_{np} - \sigma_{pp}.\end{aligned}$$

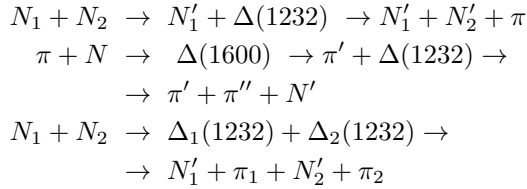
The same decomposition can be shown to apply for the elastic and the reaction cross sections too.

The cross section for pion–nucleon scattering is dominated by the existence of several direct resonances, the most prominent one being the $\Delta(1232)$. Given the pion isotopic spin ($T = 1$), the three π charge states correspond to the three values of T_z . Thus, in the pion–nucleon system two values of T are allowed: $T = \frac{1}{2}$ and $T = \frac{3}{2}$, and two independent scattering amplitudes, $A_{\frac{1}{2}}$ and $A_{\frac{3}{2}}$, enter in the cross sections. Using Clebsch-Gordan coefficients all differential cross sections can be derived from the three measured ones: $\sigma(\pi^+p \rightarrow \pi^+p)$, $\sigma(\pi^-p \rightarrow \pi^-p)$, and $\sigma(\pi^-p \rightarrow \pi^0n)$.

As soon as particle production is concerned (inelastic hadron-nucleon interactions), the description becomes immediately more complex. Two families of models are adopted, depending on the projectile energy: those based on individual resonance production and decays, which cover the energy range up to 3–5 GeV, and those based on quark/parton string models, which can provide reliable results up to several tens of TeV.

2.1. h-N interactions at intermediate energies

The inelastic channel with the lowest threshold, single pion production, opens already around 290 MeV in nucleon-nucleon interactions, and becomes important above 700 MeV. In pion-nucleon interactions the production threshold is as low as 170 MeV. Both reactions are normally described in the framework of the isobar model: all reactions proceed through an intermediate state containing at least one resonance. There are two main classes of reactions, those which form a resonant intermediate state (possible in π -nucleon reactions) and those which contain two particles in the intermediate state. The former exhibit bumps in the cross sections corresponding to the energy of the formed resonance. Examples are reported below:



Partial cross sections can be obtained from one-boson exchange theories and/or folding of Breit-Wigner with matrix elements fixed by N–N scattering or experimental data. Resonance energies, widths, cross sections, and branching ratios are extracted from data and conservation laws, whenever possible, making explicit use of spin and isospin relations. They can be also inferred from inclusive cross sections when needed.

For a discussion of resonance production, see for example [5, 6, 7].

2.2. Inelastic h-N interactions at high energies

As soon as the projectile energy exceeds a few GeV, the description in terms of resonance production and decay becomes more and more difficult. The number of resonances which should be considered grows exponentially and their properties are often poorly known. Furthermore, the assumption of one or two resonance

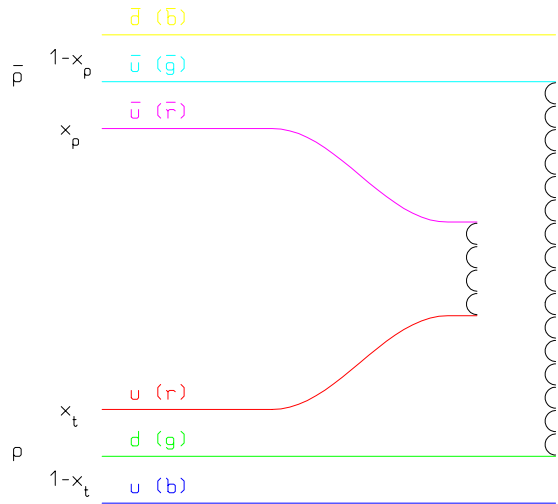


Figure 1: Leading two-chain diagram in DPM for $\bar{p} - p$ scattering. The colour (r→red, b→blue, g→green, \bar{r} →antired, \bar{b} →antiblue and \bar{g} →antigreen) and quark combination shown in the figure is just one of the allowed possibilities.

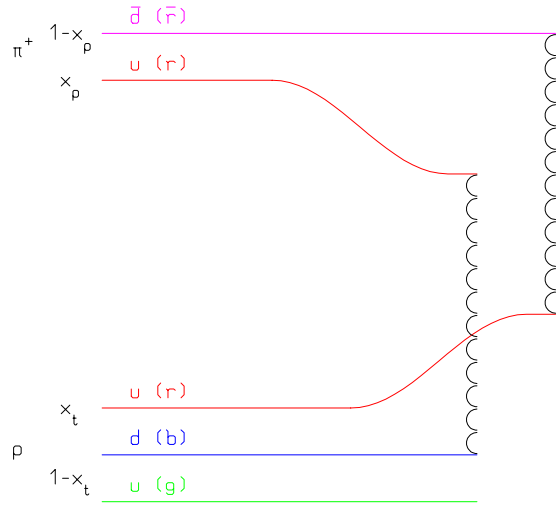


Figure 2: One of leading two-chain diagrams in DPM for $\pi^+ - p$ scattering. The colour and quark combination shown in the figure is just one of the allowed ones.

creation is unable to reproduce the experimental finding that most of the particle production at high energies occurs neither in the projectile nor in the target fragmentation region, but rather in the central region, for small values of Feynman x variable. Different models, based directly on quark degrees of freedom, must be introduced.

The features of “soft” interactions (low- p_T interac-

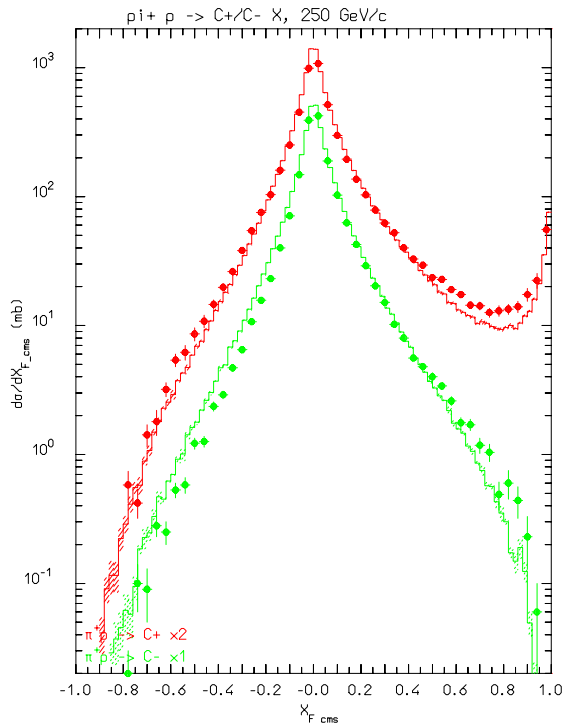


Figure 3: Feynman x_F^* spectra of positive and negative particles from (π^+, p) at 250 GeV/c. Exp. data (symbols) from [8].

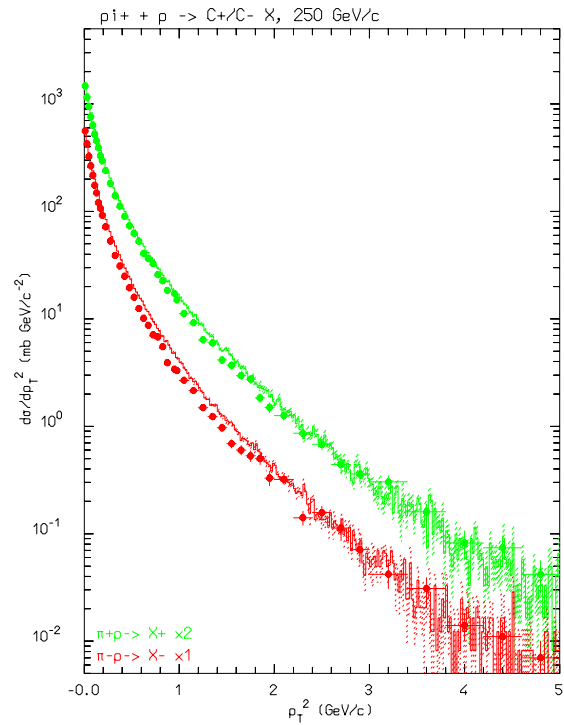


Figure 4: Transverse momentum (p_t) spectra of positive and negative particles from (π^+, p) at 250 GeV/c. Exp. data (symbols) from [8].

tions) cannot be derived from the QCD Lagrangian, because the large value taken by the running coupling constant prevents the use of perturbation theory. Models based on interacting strings have emerged as a powerful tool in understanding QCD at the soft hadronic scale, that is in the non-perturbative regime. An interacting string theory naturally leads to a topological expansion. The Dual Parton Model (DPM) [9] is one of these models and it is built introducing partonic ideas into a topological expansion which explicitly incorporates the constraints of duality and unitarity, typical of Regge's theory. In DPM hadrons are considered as open strings with quarks, antiquarks or diquarks sitting at the ends; mesons (colourless combination of a quark and an antiquark $q\bar{q}$) are strings with their valence quark and antiquark at the ends. At sufficiently high energies the leading term in the interactions corresponds to a Pomeron (IP) exchange (a closed string exchange), which has a cylinder topology. When an unitarity cut is applied to the cylindrical Pomeron, two hadronic chains are left as the sources of particle production. As a consequence of colour exchange in the interaction, each colliding hadron splits into two coloured system, one carrying colour charge c and the other \bar{c} . The system with colour charge c (\bar{c}) of one hadron combines with the system of complementary colour of the other hadron, to form two colour neutral chains. These chains appear as two back-to-back jets in their own centre-of-mass systems.

The exact way of building up these chains depends on the nature of the projectile-target combination (baryon-baryon, meson-baryon, antibaryon-baryon, meson-meson): examples are shown in figs. 1 and 2. Further details can be found in the original DPM references [9] or in [3].

The chains produced in an interaction are then hadronized. DPM gives no prescriptions on this stage of the reaction. All the available chain hadronization models, however, rely on the same basic assumptions, the most important one being *chain universality*, that is chain hadronization does not depend on the particular process which originated the chain, and until the chain energy is much larger than the mass of the hadrons to be produced, the fragmentation functions (which describe the momentum fraction carried by each hadron) are the same. As a consequence, fragmentation functions can in principle be derived from hard processes and e^+e^- data and the same functions and (few) parameters should be valid for all reactions and energies; actually mass and threshold effects are non-negligible at the typical chain energies involved in hadron-nucleus reactions. Transverse momentum is usually added according to uncertainty considerations. The examples in figs. 3 and 4 show the ability of the FLUKA model, based on DPM, to reproduce the features of particle production; further examples can be found in [1, 3].

3. Main steps of hadron–nucleus interactions

High energy hadron–nucleus (h–A) interactions can be schematically described as a sequence of the following steps:

- Glauber–Gribov cascade
- (Generalized) IntraNuclear cascade ((G)INC)
- Preequilibrium emission
- Evaporation/Fragmentation/Fission and final deexcitation

3.1. The Glauber–Gribov cascade and the formation zone

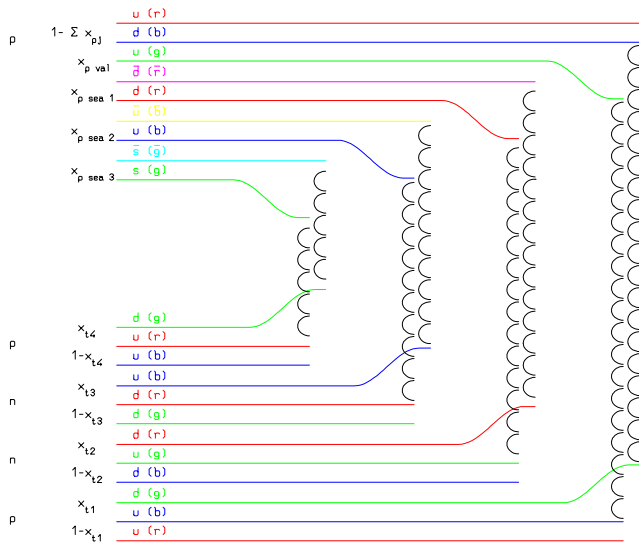


Figure 5: Leading two-chain diagrams in DPM for p – A Glauber scattering with 4 collisions. The colour and quark combinations shown in the figure are just one of the allowed possibilities.

The Glauber formalism [10, 11] provides a powerful and elegant method to derive elastic, quasi-elastic and absorption h–A cross sections from the free h–N cross section and the nuclear ground state *only*. Inelastic interactions are equivalent to multiple interactions of the projectile with ν target nucleons. The number of such “primary” interactions follows a binomial distribution (at a given impact parameter, b):

$$P_{r\nu}(b) \equiv \binom{A}{\nu} P_r^\nu(b) [1 - P_r(b)]^{A-\nu}$$

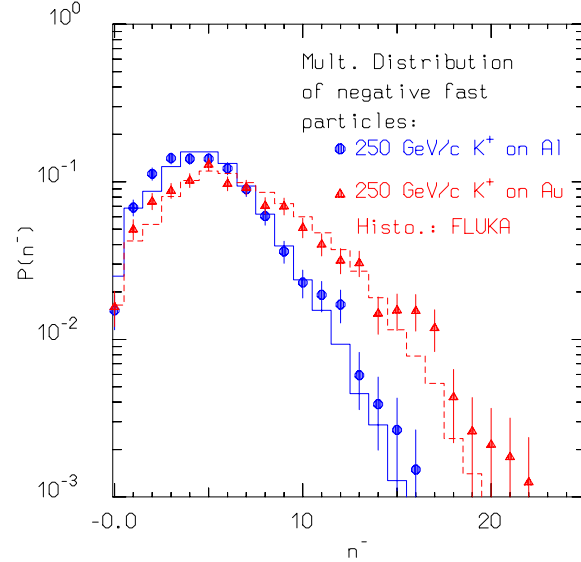


Figure 6: Multiplicity distribution of negative shower particles for 250 GeV/c K^+ on aluminium and gold targets. Data from [15].

where $P_r(b) \equiv \sigma_{hNr} T_r(b)$, and $T_r(b)$ is the profile function (folding of nuclear density and scattering profiles along the path). On average:

$$\langle \nu \rangle = \frac{Z\sigma_{hpr} + N\sigma_{hnr}}{\sigma_{hAabs}}$$

$$\sigma_{hAabs}(s) = \int d^2\vec{b} \left[1 - (1 - \sigma_{hNr}(s) T_r(b))^A \right].$$

The Glauber–Gribov model [12, 13, 14] represents the diagram interpretation of the Glauber cascade. The ν interactions of the projectile originate 2ν chains, out of which 2 chains (valence–valence chains) struck between the projectile and target valence (di)quarks, $2(\nu - 1)$ chains (sea–valence chains) between projectile sea $q - \bar{q}$ and target valence (di)quarks.

A pictorial example of the chain building process is depicted in fig. 5 for p – A : similar diagrams apply to π – A and \bar{p} – A respectively.

The distribution of the projectile energy among many chains naturally softens the energy distributions of reaction products and boosts the multiplicity with respect to hadron–hadron interactions. The building up of the multiplicity distribution from the multiple collisions can be appreciated from fig. 6, where the multiplicity distribution for Al and Au targets at 250 GeV/c are presented together. In this way, the model accounts for the major A-dependent features

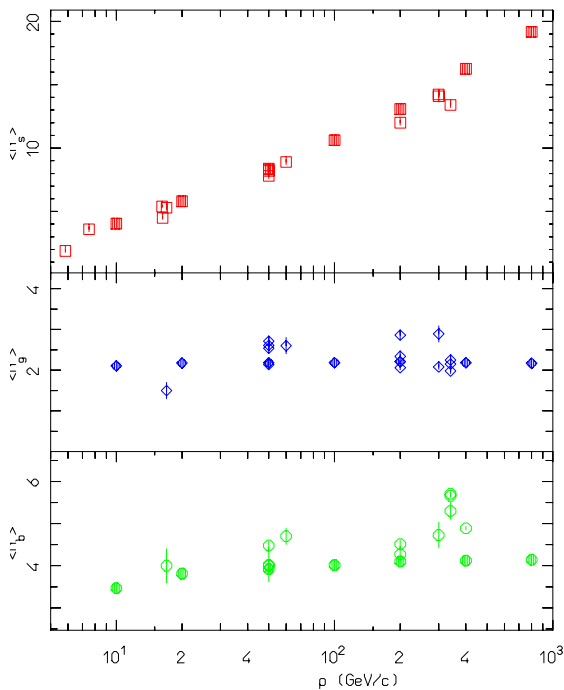


Figure 7: Shower, grey, and black tracks multiplicities for π^- on emulsion, as a function of the projectile momentum. Open symbols are experimental data from various sources, full symbols are FLUKA results.

without any degree of freedom, except in the treatment of mass effects at low energies.

The Fermi motion of the target nucleons must be included to obtain the correct kinematics, in particular the smearing of p_T distributions. All nuclear effects on the secondaries are accounted for by the subsequent (G)INC.

The *formation zone* concept is essential to understand the observed reduction of the re-interaction probability with respect of the naive free cross section assumption. It can be understood as a “materialization” time. At high energies, the “fast” (from the emulsion language) particles produced in the Glauber cascade have a high probability to materialize already outside the nucleus without triggering a secondary cascade. Only a small fraction of the projectile energy is thus left available for the INC and the evaporation.

The Glauber cascade and the formation zone act together in reaching a regime where the “slow” part of the interaction is almost independent of the particle energy. This can be easily verified looking at charged particle average multiplicities and multiplicity distributions as a function of energy (fig. 7). “Fast” (or “shower”) tracks (charged particles with $\beta = \frac{v}{c} > 0.7$), coming from the projectile primary interactions, show the typical \approx logarithmic increase observed for h–N interactions. As shown already in fig. 6, the average multiplicity and its variance are directly related

to the distribution of primary collisions as predicted by the Glauber approach. Due to the very slow variation of h–N cross section from a few GeV up to a few TeV, the Glauber cascade is almost energy independent and the rise in the multiplicity of “fast” particles is related only to the increased multiplicity of the elementary h–N interactions.

Due to the onset of formation zone effects, most of the hadrons produced in the primary collisions escape from the nucleus without further reinteractions. Further cascading only involves the slow fragments produced in the target fragmentation region of each primary interaction, and therefore it tends quickly to saturate with energy as the Glauber cascade reaches its asymptotic regime. This trend is well reflected in the average multiplicity (and multiplicity distribution) of “gray” tracks (charged particles with $0.3 < \beta < 0.7$), which are mostly protons produced in secondary collisions during the INC and preequilibrium phases.

At the end of the cascading process, the residual excitation energy is directly related to the number of primary and secondary collisions which have taken place. Each collision is indeed leaving a “hole” in the Fermi sea which carries an excitation energy related to its depth in the Fermi sea. Evaporation products, as well as residual excitation functions, should reach an almost constant condition as soon as the Glauber mechanism and the formation zone are fully developed. This can actually be verified by looking at the production of “black” tracks (charged particles with $\beta < 0.3$), which are mostly evaporation products. The data reported in fig. 7 do indeed demonstrate how they saturate as well, and how this property is well reproduced on the basis of the outlined assumptions.

3.2. (Generalized) IntraNuclear cascade

At energies high enough to consider coherent effects as corrections, a h–A reaction can be described as a cascade of two-body interactions, concerning the projectile and the reaction products. This is the mechanism called IntraNuclear Cascade (INC). INC models were developed already at the infancy of the computer era with great success in describing the basic features of nuclear interactions in the 0.2–2 GeV range. Modern INC models had to incorporate many more ideas and effects in order to describe in a reasonable way reactions at higher and lower energies. Despite particle trajectories are described classically, many quantum effects have to be incorporated in these (G)INC models, like Pauli blocking, formation time, coherence length, nucleon antisymmetrization, hard core nucleon correlations. A thorough description of the (G)INC model used in FLUKA can be found in [1, 3].

3.3. Preequilibrium

At energies lower than the π production threshold a variety of preequilibrium models have been developed [16] following two leading approaches: the quantum-mechanical multistep model and the exciton model. The former has a very good theoretical background but is quite complex, while the latter relies on statistical assumptions, and it is simple and fast. Exciton-based models are often used in Monte Carlo codes to join the INC stage of the reaction to the equilibrium one.

In the FLUKA implementation the INC step goes on until all nucleons are below a smooth threshold around 50 MeV, and all particles but nucleons (typically pions) have been emitted or absorbed. At the end of the INC stage a few particles may have been emitted and the input configuration for the preequilibrium stage is characterized by the total number of protons and neutrons, by the number of particle-like excitons (nucleons excited above the Fermi level), and of hole-like excitons (holes created in the Fermi sea by the INC interactions), and by the nuclear excitation energy and momentum. All the above quantities can be derived by properly recording what occurred during the INC stage. The exciton formalism of FLUKA follows that of M. Blann and coworkers [17, 18, 19, 20], with some modifications detailed in [3].

3.4. Evaporation, fission and nuclear break-up

At the end of the reaction chain, the nucleus is a thermally equilibrated system, characterized by its excitation energy. This system can “evaporate” nucleons, fragments, or γ rays, or can even fission, to dissipate the residual excitation.

Neutron emission is favoured over charged particle emission, due to the Coulomb barrier, especially for medium-heavy nuclei. Moreover, the excitation energy is higher in heavier nuclei due to the larger cascading chances and to the larger number of primary collisions in the Glauber cascade at high energies. The level density parameter $a \approx A/8 \text{ MeV}^{-1}$ is higher too, thus the average neutron energy is smaller. Therefore, the neutron multiplicity is higher for heavy nuclei than for light ones.

The FLUKA evaporation module is based on the standard Weisskopf-Ewing formalism [21]. Latest improvements [1] are represented by: i) adopted state density expression $\rho \propto \exp(2\sqrt{aU})/U^{\frac{5}{4}}$ (where U is the emitting nucleus excitation energy), ii) no Maxwellian approximation for energy sampling, iii) competition with γ emission, iv) sub-barrier emission. Neutron and proton production are marginally affected, while residual nuclei production and alpha emission are nicely improved.

For light residual nuclei, where the excitation energy may overwhelm the total binding energy, a statistical fragmentation (Fermi Break-up) model is more appropriate (see [1, 3, 22] for the FLUKA implementation).

The evaporation/fission/break-up processes represent the last stage of a nuclear interaction and are responsible for the exact nature of the residuals left after the interactions. However, for a coherent self-consistent model, the mass spectrum of residuals is highly constrained by the excitation energy distribution found in the slow stages, which in turn is directly related to the amount of primary collisions and following cascading which has taken place in the fast stages.

4. Nucleus–nucleus collisions

The FLUKA implementation of suitable models for heavy ion nuclear interactions has reached an operational stage. At medium/high energy (above a few GeV/n) the DPMJET model is used as described in Subsection 4.1. The major task of incorporating heavy ion interactions from a few GeV/n down to the threshold for inelastic collisions is also progressing and promising results have been obtained using a modified version of the RQMD-2.4 code (see Subsection 4.2).

4.1. The FLUKA - DPMJET interface

DPMJET-II.53 [23], a Monte Carlo model for sampling h–h, h–A and nucleus–nucleus (A–A) collisions at accelerator and cosmic ray energies (E_{lab} from 5-10 GeV/n up to 10^9 - 10^{11} GeV/n) was adapted and interfaced to FLUKA. FLUKA implements DPMJET-II.53 as an event generator to simulate A–A interactions exclusively. DPMJET (as well as the FLUKA high energy h–A generator) is based on the Dual Parton Model in connection with the Glauber formalism. The implementation of DPMJET is also considered a possible, future option to extend the FLUKA energy limits for hadronic simulations in general.

Internally, DPMJET uses Glauber impact parameter distributions per projectile–target combination. These are either computed during initialization of the program or can be processed and output in a dedicated run of DPMJET in advance. The computations are CPU intensive for heavier colliding nuclei and it would not be practical to produce the required distributions repeatedly while processing full showers in FLUKA. Therefore, a procedure was devised to efficiently provide pre-computed impact parameter distributions for a complete matrix of projectile–target combinations up to a mass number $A=246$ over the whole available energy range [24].

FLUKA requires A–A reaction cross sections internally in order to select A–A interactions appropriately. Hence, a complete matrix of A–A reaction cross sections was prepared along with the Glauber impact parameter distributions. Owing to the well established validity of the Glauber formalism, these cross sections can be safely applied down to a projectile kinetic energy ≈ 1 GeV/n.

DPMJET is called once per A–A interaction. A list of final state particles is returned by DPMJET for transport to FLUKA, as well as up to two excited residual nuclei with their relevant properties. De-excitation and evaporation of the excited residual nuclei is performed by calling the FLUKA evaporation module.

Work to interface DPMJET-III [25] is in progress.

4.2. The FLUKA - RQMD interface

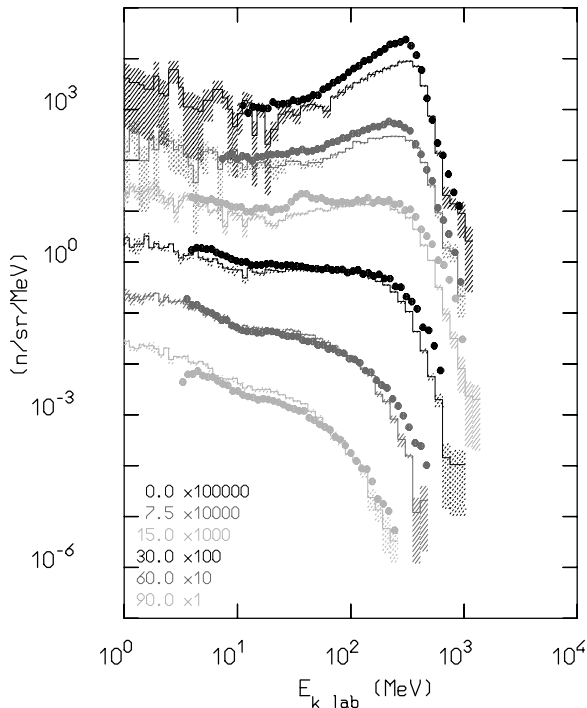


Figure 8: Double differential neutron yield by 400 MeV/n Ar ions on thick Al targets. Data are shown for six different laboratory emission angles, with the most forward on top: histograms are FLUKA results, dots experimental data [26].

Quantum Molecular Dynamics (QMD) approaches are a viable solution for A–A reactions. They represent an improvement over classical INC codes, thanks to their dynamic modelling of the nuclear field among nucleons during the reaction. The treatment of individual two-body scattering/interactions is usually based on similar approaches for INC and QMD codes.

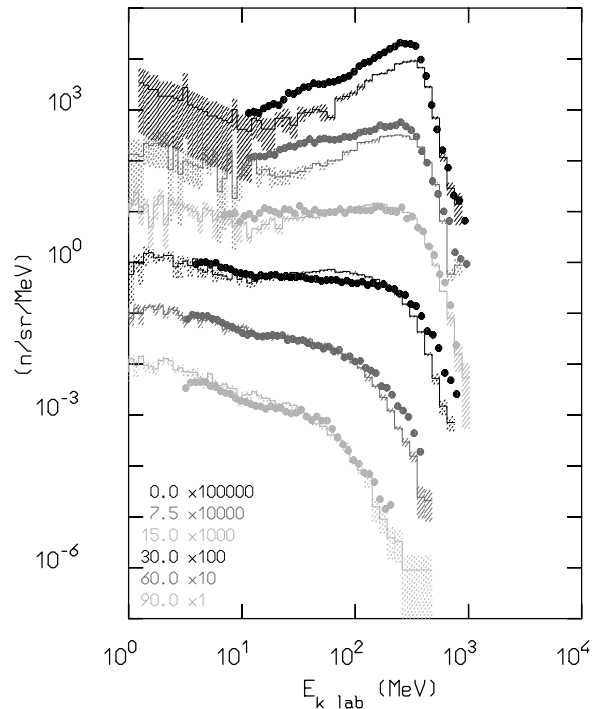


Figure 9: The same as fig. 8 for Fe ions.

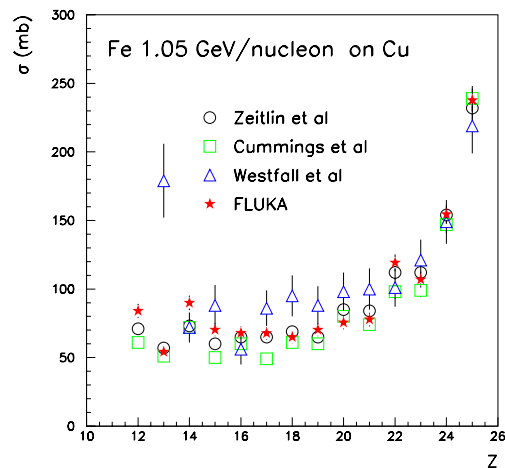


Figure 10: Fragment charge cross sections for 1.05 GeV/n Fe ions on Cu. Stars FLUKA, circles [27], squares (1.5 GeV/n) [28], triangles (1.88 GeV/n) [29].

Unfortunately, initialization of the projectile and target nuclear states is often difficult and their relativistic extension somewhat problematic.

The RQMD-2.4 [30, 31] is a relativistic QMD model which has been applied successfully to relativistic A–A particle production over a wide energy range, from ≈ 0.1 GeV/n up to several hundreds of GeV/n. The

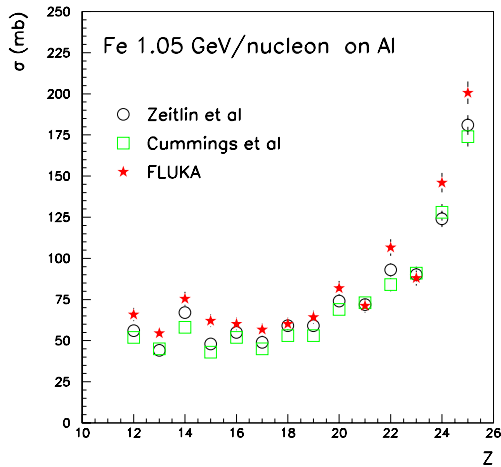


Figure 11: The same as fig. 10 for 1.05 GeV/n Fe ions on Al.

high energy A–A part in FLUKA is already successfully covered by DPMJET. For energies below a few GeV/n several models are under development, either new (see Section 5), or based on the extension of the present intermediate energy h–A model of FLUKA. However, a RQMD-2.4 interface has been developed meanwhile to enable FLUKA to treat ion interactions from ≈ 100 MeV/n up to 5 GeV/n where DPMJET starts to be applicable.

Several important issues had to be addressed. RQMD does not identify nuclei in the final state. Hence, no low energy de-excitation (evaporation, fragmentation...) is performed for neither the excited projectile nor the target residues. This is highly problematic, particularly for the projectile residue, since its de-excitation usually gives rise to the highest energy particle production in the laboratory frame. Serious energy non-conservation issues are also affecting the code, particularly when run in full QMD mode (RQMD can be run both in full QMD mode and in the so called “fast cascade” mode where it behaves as an INC code). Therefore a meaningful calculation of residual excitation energies was impossible with original code.

The adopted solution was to modify the code, reworking the nuclear final state out of the available information on spectators, correlating the excitation energy to the actual depth of holes left by hit nucleons. Finally, the remaining energy-momentum conservation issues were resolved taking into account experimental binding energies, as in all other FLUKA models. After these improvements a meaningful excitation energy could be computed and the FLUKA evaporation model (see Subsection 3.4) was used to produce the particles of low energy (in their respec-

tive rest frames) emitted by the excited projectile and target residues.

Examples of the performances of FLUKA when run with the modified RQMD-2.4 code are presented in figs. 8, 9, 10, and 11 and compared with experimental data, for double differential neutron production at 400 MeV/n and fragment production at 1.05 GeV/n.

5. Perspectives

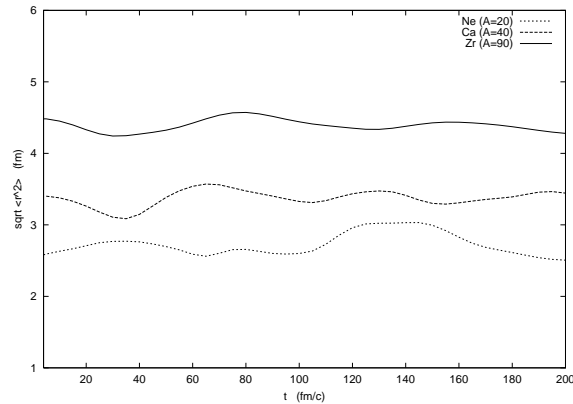


Figure 12: Root mean square radii (fm) of selected ^{20}Ne , ^{40}Ca , ^{90}Zr initial nuclear configurations versus time (fm/c).

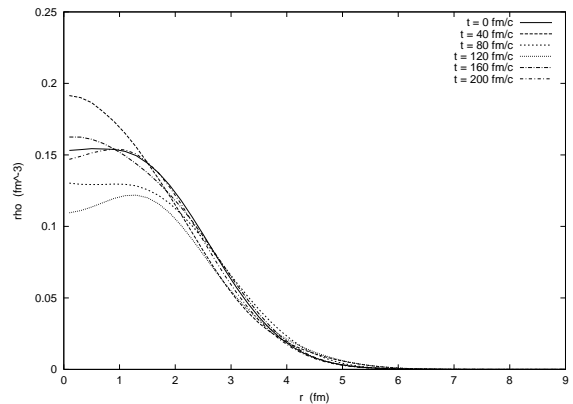


Figure 13: Radial spatial density profile of the same ^{20}Ne configuration shown in fig. 12, at the beginning of the time evolution (solid line) and at subsequent times ($\Delta t = 40$ fm/c).

A new QMD code is also being developed from scratch to describe A–A collisions taking into account both the effect of stochasting scattering between all the nucleons involved and the effect of the nuclear potential which acts on each nucleon. Protons and neutrons are described as gaussian wave packets of

fixed widths; the total nuclear wave function is approximated by the product of single nucleon wave functions. Regarding the Hamiltonian, each group of QMD model developers makes its particular choices (see, for instance, refs. [30, 32, 33, 34, 35, 36]); our starting point is a non-relativistic phenomenological potential, based on Skyrme interaction, supplemented by surface and symmetry terms; we add also the electromagnetic repulsion between protons, crucial to determine low-energy nuclear trajectories. In principle one can build an Hamiltonian as sophisticated as desired to improve the nuclear physical description; in practice however one has to meet CPU time requirements.

The parameters of the model are fixed in order to reproduce as accurately as possible the observed nuclear ground state properties. We emphasize that this result can be achieved only approximatively, because one has to describe with only a few parameters a great variety of nuclei, ranging from the lightest to the heaviest ones. For this purpose a gaussian width increasing with increasing mass number turns out to be useful, as suggested for instance in [35]. On the other hand, taking a gaussian width which differs from nucleon to nucleon and evolves in time, as done for instance in [37], is practicable only for light nuclei; for the intermediate mass and heavy ones the required CPU time becomes higher and higher.

We underline that QMD codes are based on Monte Carlo simulations: the cross-sections for A–A interactions are obtained as mean values from hundreds and hundreds of events, each of which should involve different starting nuclear configurations. In practice, it turns out that one can simulate a wide variety of different events with only a few initial configurations, randomly rotated.

Reasonable initial configurations can be chosen and stored. The time evolution of root mean square radii for selected ^{20}Ne , ^{40}Ca , ^{90}Zr configurations is shown in fig. 12; the rms radii slightly oscillate with time because the nucleons are not frozen inside the nucleus: each of them moves in the potential well originated from all the others because of its Fermi momentum, different from zero. Note that QMD initial configurations are not classical Hamiltonian minima, which would break the Pauli principle [34]. One has to make sure that no nucleons escape at least for a time of the order of that required to A–A collisions to take place (\sim hundreds of fm/c); only configurations which do not originate this spurious emission are selected and stored for subsequent simulations.

The stored configurations should also provide reasonable values for density and momentum distributions.

The radial spatial density profile is plotted in fig. 13 for the same ^{20}Ne nucleus whose root mean square radius evolution is shown in fig. 12; each curve refers to a different time during evolution. One can see that,

as well as the radius, also the density oscillates around its typical mean value. Similar plots can be obtained for the time evolution of the momentum distribution.

It is planned to couple the dynamical nuclear evolution predicted by our QMD, which gives the description of the first stage of the reaction, with the FLUKA preequilibrium module, to describe the de-excitation of the fragments formed and to study deeply the fragmentation process, implementing suitable models.

Moreover, a promising task is represented by the coupling of FLUKA with a Monte Carlo code [38] developed at Milan University and based on Boltzmann Master Equation theory, as a tool to treat ion–ion interactions below 100 MeV/n.

Acknowledgments

This work was partially supported under NASA Grant NAG8-1658, ASI contract 1/R/320/02, and EC contract FIGH-CT1999-00005.

References

- [1] A. Fassò, A. Ferrari, J. Ranft, and P.R. Sala, *New Developments in FLUKA Modelling of Hadronic and EM Interactions*, in Proceedings of SARE-3, KEK-Tsukuba, H. Hirayama ed., May 7–9 1997, KEK report Proceedings 97-5, 32 (1997).
- [2] A. Fassò, A. Ferrari, J. Ranft, and P.R. Sala, *FLUKA: Status and Prospective for Hadronic Applications*, in Proceedings of the Monte Carlo 2000 Conference, Lisbon, October 23–26 2000, A. Kling, F. Barão, M. Nakagawa, L. Távara, P. Vaz eds., Springer-Verlag Berlin, 955 (2001).
- [3] A. Ferrari, and P.R. Sala, *The Physics of High Energy Reactions*, in Proceedings of Workshop on Nuclear Reaction Data and Nuclear Reactors Physics, Design and Safety, A. Gandini, G. Reffo eds., Trieste, Italy, April 1996, **2**, 424 (1998).
- [4] A. Ferrari and P.R. Sala, *Nuclear Reactions in Monte Carlo Codes*, in Radiation Protection Dosimetry, R. Cherubini, D.T. Goodhead, H.G. Menzel, A. Ottolenghi eds., Nuclear Technology Publishing, Vol. **99**, Nos 1–4, 29 (2002).
- [5] S. Huber, and J. Aichelin, *Production of Δ - and N^* - resonances in the one-boson exchange model*, Nucl. Phys. **A573**, 587 (1994).
- [6] A. Engel, W. Cassing, U. Mosel, M. Schäfer, Gy. Wolf, *Pion-nucleus reactions in a microscopic transport model*, Nucl. Phys. **A572**, 657 (1994).
- [7] S. Teis, W. Cassing, M. Effenberger, A. Hombach, U. Mosel, Gy. Wolf, *Pion-production in heavy-ion collisions at SIS energies*, Z. Phys. A **356**, 421 (1997).

- [8] M. Adamus and 40 others, *Charged particle production in K^+p , π^+p and pp interactions at 250 GeV/c*, Z. Phys. **C39**, 311 (1988).
- [9] A. Capella, U. Sukhatme, C.-I. Tan and J. Tran Thanh Van, *Dual Parton Model*, Phys. Rep. **236**, 225 (1994).
- [10] R.J. Glauber and G. Matthiae, *High-energy scattering of protons by nuclei*, Nucl. Phys. **B21**, 135 (1970).
- [11] R.J. Glauber, *High-energy Collision Theory*, in *Lectures in Theoretical Physics*, A.O. Barut, and W.E. Brittin eds, Interscience, NewYork (1959).
- [12] V.N. Gribov, *Glauber corrections and the interaction between high-energy hadrons and nuclei*, Sov. Phys. JETP **29**, 483 (1969).
- [13] V.N. Gribov, *Interaction of gamma quanta and electrons with nuclei at high energies*, Sov. Phys. JETP **30**, 709 (1970).
- [14] L. Bertocchi, *Graphs and Glauber*, Nuovo Cimento **11A**, 45 (1972).
- [15] I.V. Ajinenko and 40 others, *Multiplicity distribution in K^+Al and K^+Au collisions at 250 GeV/c and a test of the multiple collision model*, Z. Phys. **C42**, 377 (1989).
- [16] E. Gadioli, and P.E. Hodgson, *Pre-equilibrium Nuclear Reactions*, Clarendon Press, Oxford, (1992).
- [17] M. Blann, *Hybrid model for pre-equilibrium decay in nuclear reactions*, Phys. Rev. Lett. **27**, 337 (1971).
- [18] M. Blann, *Importance of the nuclear density distribution on pre-equilibrium decay*, Phys. Rev. Lett. **28**, 757 (1972).
- [19] M. Blann and H.K. Vonach, *Global test of modified precompound decay models*, Phys. Rev. **C28**, 1475 (1983).
- [20] M. Blann, *Precompound analyses of spectra and yields following nuclear capture of stopped π^-* , Phys. Rev. **C28**, 1648 (1983).
- [21] V.F. Weisskopf, *Statistics and nuclear reactions*, Phys. Rev. **52**, 295 (1937).
- [22] A. Ferrari, P.R. Sala, J. Ranft, and S. Roesler, *Cascade particles, nuclear evaporation, and residual nuclei in high energy hadron-nucleus interactions*, Z. Phys. **C70**, 413 (1996).
- [23] J. Ranft, *Dual Parton Model at cosmic ray energies*, Phys. Rev. **D51**, 64 (1995).
- [24] A. Empl, A. Fassò, A. Ferrari, *et al.*, *Progress and Applications of FLUKA*, Proc. ANS Radiation Protection & Shielding Division 12th Topical Meeting, Santa Fe, New Mexico, USA, April 14–18 2002, (6 pages, published in electronic format)
- [25] S. Roesler, R. Engel and J. Ranft, *The Monte Carlo Event Generator DPMJET-III*, Proc. Monte Carlo 2000 Conference, Lisbon, October 23–26 2000, A. Kling, F. Barão, M. Nakagawa, L. Távora, P. Vaz eds., Springer-Verlag Berlin, 1033 (2001).
- [26] T. Kurosawa, N. Nakao, T. Nakamura, *et al.*, *Neutron yields from thick C, Al, Cu and Pb targets bombarded by 400 MeV/nucleon Ar, Fe, Xe and 800 MeV/nucleon Si ions*, Phys. Rev. **C62**, 044615-1 (2000).
- [27] C. Zeitlin, L. Heilbronn, J. Miller, *et al.*, *Heavy fragment production cross sections from 1.05 GeV/nucleon ^{56}Fe in C, Al, Cu, Pb and CH_2 targets*, Phys. Rev. **C56**, 388 (1997).
- [28] J. R. Cummings, W. R. Binns, T. L. Garrard, *et al.*, *Determination of the cross sections for the production of fragments from relativistic nucleus-nucleus interactions. I. Measurements*, Phys. Rev. **C42**, 2508 (1990).
- [29] G. D. Westfall, L. W. Wilson, P. J. Lindstrom, *et al.*, *Fragmentation of relativistic ^{56}Fe* , Phys. Rev. **C19**, 1309 (1979).
- [30] H. Sorge, H. Stöcker, and W. Greiner, *Poincaré invariant hamiltonian dynamics: modelling multi-hadronic interactions in a phase space approach*, Ann. of Phys. **192**, 266 (1989).
- [31] H. Sorge, *Flavor production in Pb(160 AGeV) on Pb collisions: Effect of color ropes and hadronic rescattering*, Phys. Rev. **C52**, 3291 (1995).
- [32] J. Aichelin, *Quantum Molecular Dynamics – A dynamical microscopic n-body approach to investigate fragment formation and the nuclear equation of state in heavy ion collisions*, Phys. Rep. **202**, 233 (1991).
- [33] S. R. Souza, L. de Paula, S. Leray, *et al.*, *A dynamical model for multifragmentation of nuclei*, Nucl. Phys. **A571**, 159 (1994).
- [34] K. Niita, S. Chiba, T. Maruyama, *et al.*, *Analysis of the (N, xN') reactions by quantum molecular dynamics plus statistical decay model*, Phys. Rev. **C52**, 2620 (1995).
- [35] N. Wang, Z. Li, and X. Wu, *Improved quantum molecular dynamics model and its applications to fusion reaction near barrier*, Phys. Rev. **C65**, 064608-1 (2002).
- [36] M. Papa, T. Maruyama, and A. Bonasera, *Constrained molecular dynamics approach to fermionic systems*, Phys. Rev. **C64**, 024612-1 (2001).
- [37] T. Maruyama, K. Niita, and A. Iwamoto, *Extension of quantum molecular dynamics and its application to heavy-ion collisions*, Phys. Rev. **C53**, 297 (1996).
- [38] M. Cavinato, E. Fabrici, E. Gadioli, E. Gadioli Erba, and G. Riva, *Monte Carlo calculations of heavy ion cross-sections based on the Boltzmann master equation theory*, Nucl. Phys. **A679**, 753 (2001).